

# Chromium isotopic composition of core-top planktonic foraminifera

X. L. Wang<sup>1</sup> | N. J. Planavsky<sup>1</sup> | P. M. Hull<sup>1</sup> | A. E. Tripati<sup>2,3</sup> | H. J. Zou<sup>1</sup> | L. Elder<sup>1</sup> | M. Henehan<sup>1</sup>

<sup>1</sup>Yale University, New Haven, CT, USA

<sup>2</sup>University of California, Los Angeles, CA, USA

<sup>3</sup>Université de Brest, Plouzané, France

## Correspondence

X. Wang, Yale University, New Haven, CT, USA

Email: xiangli.wang@yale.edu

## Abstract

The chromium isotope system ( $^{53}\text{Cr}/^{52}\text{Cr}$  expressed as  $\delta^{53}\text{Cr}$  relative to NIST SRM 979) is potentially a powerful proxy for the redox state of the ocean–atmosphere system, but a lack of temporally continuous, well-calibrated archives has limited its application to date. Marine carbonates could potentially serve as a common and continuous Cr isotope archive. Here, we present the first evaluation of planktonic foraminiferal calcite as an archive of seawater  $\delta^{53}\text{Cr}$ . We show that single foraminiferal species from globally distributed core tops yielded variable  $\delta^{53}\text{Cr}$ , ranging from 0.1‰ to 2.5‰. These values do not match with the existing measurements of seawater  $\delta^{53}\text{Cr}$ . Further, within a single core-top, species with similar water column distributions (i.e., depth habitats) yielded variable  $\delta^{53}\text{Cr}$  values. In addition, mixed layer and thermocline species do not consistently exhibit decreasing trends in  $\delta^{53}\text{Cr}$  as expected based on current understanding of Cr cycling in the ocean. These observations suggest that either seawater  $\delta^{53}\text{Cr}$  is more heterogeneous than previously thought or that there is significant and species-dependent Cr isotope fractionation during foraminiferal calcification. Given that the  $\delta^{53}\text{Cr}$  variability is comparable to that observed in geological samples throughout Earth's history, interpreting planktonic foraminiferal  $\delta^{53}\text{Cr}$  without calibrating modern foraminifera further, and without additional seawater measurements, would lead to erroneous conclusions. Our core-top survey clearly indicates that planktonic foraminifera are not a straightforward  $\delta^{53}\text{Cr}$  archive and should not be used to study marine redox evolution without additional study. It likewise cautions against the use of  $\delta^{53}\text{Cr}$  in bulk carbonate or other biogenic archives pending further work on vital effects and the geographic heterogeneity of the Cr isotope composition of seawater.

## 1 | INTRODUCTION

The redox state of the ocean–atmosphere system is closely linked to the availability of bioessential elements (e.g., Fe, N and P) and plays a key role in shaping ecosystem structure (Hutchins & Bruland, 1998; Keeling, Körtzinger, & Gruber, 2010; Lenton & Watson, 2000; Silvester, 1989; Van Cappellen & Ingall, 1996). Therefore, redox records are needed to gain a full understanding of the evolution of biogeochemical cycles and the role that environmental factors have played

in driving large-scale ecosystem shifts in Earth history. Metal isotopes have recently emerged as a key part of our toolkit for tracking marine redox evolution. An important step toward the meaningful application of these metal isotope proxies, however, is to determine what sedimentary archives can provide robust records of seawater chemistry. Therefore, in this study, we focus on planktonic foraminifera, marine calcifiers with a temporally continuous fossil record since Cretaceous.

The stable isotope ratios  $^{53}\text{Cr}/^{52}\text{Cr}$  could be a sensitive proxy for marine redox state. Chromium in the ocean is mainly sourced from

**TABLE 1** Full and abbreviated species names, habitat depth, and symbiosis of selected foraminifera

Full species name	Abbreviated species name	Habitat depth	Symbiont	References
<i>Trilobatus sacculifer</i>	<i>T. sacculifer</i>	Mixed layer (50 m)	Dinoflagellates	Hemleben et al., 2012
<i>Orbulina universa</i>	<i>O. universa</i>	Mixed layer/Thermocline	Dinoflagellates	Hemleben et al., 2012
<i>Pulleniatina obliquiloculata</i>	<i>P. obliquiloculata</i>	Mixed layer/Thermocline	Chryosphytes	Bé & Tolderlund, 1971
<i>Globigerinella siphonifera</i>	<i>G. siphonifera</i>	Mixed layer/Thermocline	Chryosphytes	Bé & Tolderlund, 1971
<i>Neogloboquadrina dutertrei</i>	<i>N. dutertrei</i>	Mixed layer/Thermocline	Facultative	Hemleben et al., 2012
<i>Globorotalia tumida</i>	<i>G. tumida</i>	Mixed layer/Thermocline	None	Hemleben et al., 2012
<i>Menardella menardii</i>	<i>M. menardii</i>	Mixed layer/Thermocline	Facultative	Hemleben et al., 2012
<i>Truncorotalia crassaformis</i>	<i>T. crassaformis</i>	Subthermocline	None	Bé & Tolderlund, 1971
<i>Truncorotalia truncatulinoides</i>	<i>T. truncatulinoides</i>	Subthermocline	None	Hemleben et al., 2012

rivers and primarily buried into reducing sediments (e.g., Jeandel & Minster, 1984, 1987; Martin & Meybeck, 1979; Reinhard et al., 2013). Oxidative weathering of continental rocks transforms insoluble Cr(III) (average upper continental crust [Cr] = 92 ppm, Rudnick & Gao, 2003) into soluble Cr(VI), which is then delivered to oceans by rivers. Chromium can also be transported as Cr(III) contained in detrital grains or complexed with organic ligands. These two Cr(III) transport pathways can deliver significant Cr flux to the ocean (e.g., see references in Bonnard, James, Parkinson, Connelly, & Fairchild, 2013; Konhauer et al., 2011), but they are unlikely to induce large Cr isotope variation as no redox transformation is involved (e.g., Ellis, Johnson, & Bullen, 2004; Schauble, Rossman, & Taylor, 2004; Schoenberg, Zink, Staubwasser, & Von Blanckenburg, 2008). The oxidation of Cr(III) to Cr(VI) requires manganese oxides, and manganese oxide formation, in turn, requires free oxygen–O<sub>2</sub> (e.g., Eary & Rai, 1987; Fendorf & Zasoski, 1992). Therefore, Cr isotope variation can be used as an indicator of the presence of atmospheric oxygen (e.g., Frei, Gaucher, Poulton, & Canfield, 2009). Building on this framework, Cr has been used to provide new insights on the oxygenation of the early Earth (Crowe et al., 2013; Frei et al., 2009; Planavsky, Reinhard et al., 2014).

Chromium is removed from seawater into sediments mainly through reduction of soluble Cr(VI) to insoluble Cr(III). The reduction may occur in the water column or below the sediment–water interface (Reinhard et al., 2014 and references therein), as long as there are reductants such as sulfide, ferrous iron, or anaerobic microbes (Basu & Johnson, 2012; Døssing, Dideriksen, Stipp, & Frei, 2011; Ellis, Johnson, & Bullen, 2002; Kitchen, Johnson, Bullen, Zhu, & Raddatz, 2012). Reduction leaves the remaining Cr(VI) in seawater fractionated to higher  $\delta^{53}\text{Cr}$  values, with the size of the fractionation being affected by specific reduction mechanisms and kinetics. In the simplest sense of the marine Cr isotope system, this means that as the spatial extent of reducing marine sediments expands, seawater  $\delta^{53}\text{Cr}$  will shift to higher values. Therefore, although even basic aspects of the modern Cr isotope mass balance are still being refined (e.g., Frei, Poiré, & Frei, 2014; Gueguen et al., 2016; Reinhard et al., 2014), seawater Cr isotopic composition can potentially be used to track the evolution of seawater redox conditions. Moreover, the chromium isotope system appears to be insensitive to non-redox removal processes such as sorption (Ellis et al., 2004). Therefore, interpretation of the marine Cr

isotope record could be relatively straightforward, compared to other redox proxies such as Mo isotopes that are strongly affected by non-redox processes (e.g., Barling & Anbar, 2004).

Marine carbonate sediments have been proposed as a potential archive for seawater  $\delta^{53}\text{Cr}$  (Pereira et al., 2015; Rodler, Sánchez-Pastor, Fernández-Díaz, & Frei, 2015). The appeal of carbonates is fairly obvious—they are some of the most commonly utilized paleoceanographic archives and can offer temporally continuous records. In this study, we use core-top samples to explore whether planktonic foraminifera can serve as an archive for seawater  $\delta^{53}\text{Cr}$  values over the last 150 million years. Specifically, we aim to characterize the  $\delta^{53}\text{Cr}$  values of some common foraminifera species and compare them with published seawater  $\delta^{53}\text{Cr}$ .

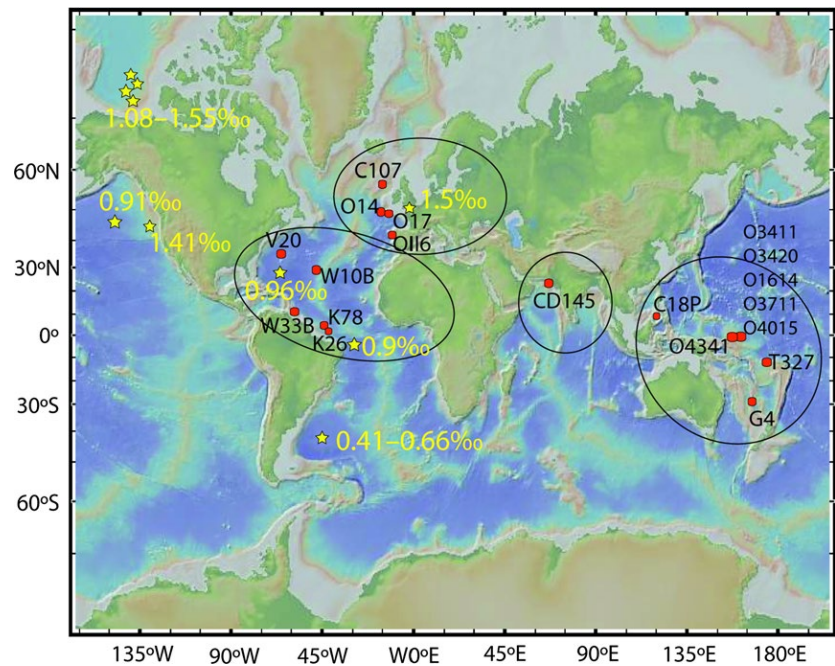
## 2 | MATERIALS AND METHODS

### 2.1 | Sampling strategy

Planktonic foraminifera are a group of free-floating protozoa with systematic depth habitat variation among species (from the surface photic zone to subthermocline depths) and with ontogeny. Found worldwide, planktonic foraminifera are a key resource in paleoceanography and paleoclimatology (Hemleben, Spindler, & Anderson, 2012). For this study, we selected planktonic foraminifera species with different habitat depths and symbiont associations (Table 1). Both these factors are known to affect isotopic fractionation in other geochemical systems including the carbon, oxygen, clumped isotope, and boron isotope systems (Henehan et al., 2013; Spero, Lerche, & Williams, 1991; Tripathi et al., 2010).

Planktonic foraminifera were picked from the uppermost 0.5 cm to 1 cm of core-top samples from the Atlantic, Arabian Sea, and Pacific (Fig. 1, Table 2). Time averaging within a 1 cm interval is ~10–20 years in hemipelagic sediments and ~100–5000 years in pelagic sediments (Müller & Suess, 1979), which is shorter than the residence time of Cr (~9000 years) in the modern ocean, so temporal variation of seawater  $\delta^{53}\text{Cr}$  should not significantly interfere with our evaluation of the  $\delta^{53}\text{Cr}$  proxy in planktonic foraminiferal calcite. Furthermore, two core-top samples, KC26 and KC78, have been constrained to be Holocene

**FIGURE 1** A map showing core-top locations and published seawater  $\delta^{53}\text{Cr}$  values. The full names of the stations are given in Table 2. Red symbols represent locations of samples in this study, while yellow symbols denote locations with published seawater values (Bonnand et al., 2013; Pereira et al., 2015; Scheiderich et al., 2015). We divided our dataset into four regions, as outlined by the ellipses: the North Atlantic, the Central Atlantic, the North Arabian Sea, and the West Pacific. For interpretation of the colors in this figure, the readers are referred to the web version of this article



or younger (Sun, Corliss, Brown, & Showers, 2006) and two samples, G4 and T327, have been dated by  $^{14}\text{C}$  method to be 945 year BP (H. C. Bostock, pers. comm.) and 4199 year BP (Cortese & Prebble, 2015), respectively. That said, core tops in some regions can contain older specimens due to sediment reworking (e.g., Sun et al., 2006). As such, we cannot rule out that temporal variation of seawater  $\delta^{53}\text{Cr}$  isotopes adds to the variability observed among some of our sites, but our major conclusions are supported based on well-dated samples.

Where necessary, bulk foraminiferal samples were separated from core-top sediments by washing and sieving in deionized water over a 63- $\mu\text{m}$  sieve, in Hull laboratory at Yale or elsewhere. Some samples (KC26, KC78, VM20-248, G4, T327) were obtained from colleagues as washed splits (R.D. Norris, Scripps Institute of Oceanography, University of California San Diego, USA; D.H. Corliss, Graduate School of Oceanography, University of Rhode Island, USA; H. Bostock, National Institute of Water and Atmospheric Research, New Zealand). For samples analyzed as 'bulk foraminifera', that is, mixed species (VM20), all non-foraminiferal materials were removed from the >125  $\mu\text{m}$  size fraction under a binocular microscope. Individual species (Fig. 2) were picked from >125  $\mu\text{m}$  size fractions until a target mass of 40–150 mg of carbonate per sample was reached. During picking, we avoided foraminiferal tests covered with dark coatings (likely metal oxides), except for the bulk foram sample VM20-248. All species were identified according to the species concepts of Kennett and Srinivasan (1983), with names updated to Aze et al. (2011) and Spezzaferri et al. (2015). P. Hull checked the accuracy of species identification before dissolution.

## 2.2 | Sample preparation and chemical separation

SeaStar acetic acid (10 ml, 1 M) at room temperature (without sonication) was used to dissolve calcite but leave clays, if any, intact (more below). Immediately after bubbling (from dissolution of calcite)

ceased, samples were centrifuged at 3000 rpm for 5 min. Leachates were transferred to 15-ml Savillex PFA beakers and evaporated to dryness on a hotplate. The dried samples were white, indicating absence of obvious organic matter. However, aqua regia ( $\text{HCl}:\text{HNO}_3 = 3:1$ ) was still added to the samples and heated at 130°C for 24 hr. Samples were again evaporated to dryness on a hotplate and dissolved in 4 ml 6 N HCl. From the 4 ml digest, a 0.05 ml aliquot was taken for element concentration measurements on a Thermo Finnigan ElementXR ICP-MS. A multi-element standard solution, made from PlasmaCal standard solutions ( $1000 \pm 5 \mu\text{g ml}^{-1}$ , SCP Science), was used to calibrate the instrument. Uncertainty of the concentration measurement is typically less than 5%.

We used a  $^{50}\text{Cr}$ - $^{54}\text{Cr}$  double spike technique (Ellis et al., 2002; Schoenberg et al., 2008) to correct for potential isotope fractionations occurring during sample preparation and measurement. Based on the measured Cr concentrations from ICP-MS, sample digests were spiked with an appropriate amount of the Cr double spike so as to achieve spike/sample ratios  $[(^{54}\text{Cr})_{\text{spike}} / (^{52}\text{Cr})_{\text{sample}}]$  of  $\sim 0.5$ . Spiked samples were slowly evaporated to dryness overnight to allow spike-sample equilibration and then taken up in 0.5 ml 6 N HCl. Samples were then left on hotplate at 100°C with lids closed for 4 hr to ensure chemical equilibrium.

Although acetic acid leaves clays intact (e.g., Hirst & Nicholls, 1958; Salomons & Förstner, 1980), it can potentially release Cr adsorbed to the surface of clay particles. We tested this possibility on a subset of samples (Table 3), by measuring the Cr content of pure water rinses. In these tests, foraminiferal chambers were opened by gently crushing—without pulverizing—between two class slides (Fig. 2J). The opened chambers were rinsed twice with 18.2 M $\Omega$  water (Milli-Q, Millipore), with 30 s sonication during each rinse. The two rinses were combined and measured for the total Cr mass.

Due to the very low Cr levels in foraminiferal calcite ( $0.06 \mu\text{g g}^{-1}$  to  $0.8 \mu\text{g g}^{-1}$ ; see the Result section), we used a low-blank ( $<1 \text{ ng}$ )

**TABLE 2** Basic information, Cr isotopic composition, and Cr-Ti concentrations for the foraminiferal species (Table 1) investigated. The abbreviated labels are used in Figs. 1 and 5

Abbreviated Label	Original sample label	Species	Yale Peabody Museum #	Core-top Water depth (m)	Latitude	Longitude	$\delta^{53}\text{Cr}$ (‰)	2 sigma internal <sup>a</sup>	53Cr blank corr. (%)	2 sigma external <sup>a</sup>	53Cr clay (%)	2 sigma internal	Total Cr (ng) used	Cr Yield <sup>b</sup>	Cr (ID) <sup>c</sup> ( $\mu\text{g g}^{-1}$ )	Cr (ICP-MS) ( $\mu\text{g g}^{-1}$ )	Ti (ICP-MS) ( $\mu\text{g g}^{-1}$ )	Cr/Mn
Central atlantic																		
W33B	WIND 33B	<i>T. sacculifer</i> (Sacless)		3520	11.2118	-58.7707	0.61	0.09	0.62	0.26	-0.11	0.06	7.6	85%	0.39	0.41	1.07	0.020
W10B	WIND 33B#	<i>T. sacculifer</i> (Sacless)		3520	11.2118	-58.7707	0.37	0.09	0.37	0.26			8.5	76%	0.38			0.006
K26	WIND 10B	<i>T. sacculifer</i> (Sac)		2871	29.1248	-47.549	0.62	0.29	0.65	0.26	-0.17	0.05	3.9	51%	0.20	0.18	1.14	0.006
	KC26	<i>T. sacculifer</i> (mixed)	307871	3772	5.457	-44	0.32	0.09	0.31	0.26			11.0	56%	0.12	0.13	0.17	0.002
	KC26	<i>G. tumida</i>	307872	3772	5.457	-44	0.41	0.05	0.41	0.26			25.9	55%	0.31	0.13	0.32	0.002
	KC26	<i>M. menardii</i>	307873	3772	5.457	-44	0.16	0.10	0.14	0.26			5.9	77%	0.06	0.06	0.10	0.001
	KC26	<i>O. universa</i>	307874	3772	5.457	-44	1.07	0.09	1.10	0.26			11.3	56%	0.26	0.18	0.06	0.005
K78	KC78	<i>O. universa</i>	307869	3273	5.267	-44.133	0.87	0.08	0.91	0.26	-0.12	0.06	6.7	65%	0.18	0.20	0.55	0.003
V20	VM20-248	Bulk foram	307867	1575	33.5	-64.4	0.56	0.07	0.56	0.26			19.7	64%	0.18	0.19	0.07	0.002
North Atlantic																		
O14	OMEX 14B	<i>O. universa</i>		3656	48.9988	-13.2087	0.36	0.18	0.36	0.26	-0.19	0.05	6.8	51%	0.12	0.16	0.55	0.005
O16	OMEX II 6B	<i>O. universa</i>		2900	41.8012	-10.1185	0.38	0.12	0.38	0.26	0.03	0.06	7.2	83%	0.16	0.17	0.32	0.003
O17	OMEX I 17B	<i>O. universa</i>		1475	48.9169	-11.8348	0.56	0.08	0.57	0.26	-0.13	0.06	12.9	33%	0.30	0.25	0.47	0.004
C107	CD107 A MC 4A	<i>O. universa</i>		3569	57	-15	0.85	0.37	0.92	0.44	-0.09	0.12	3.4	48%	0.10	0.11	1.21	0.003
West Pacific																		
O3411	OJP3411	<i>P. obliquiloculata</i>		3411	0	161	0.30	0.33	0.29	0.39			3.2	51%	0.09	0.10	0.85	0.003
	MW0691 4BC51																	
O1614	OJP1614 1BC7	<i>P. obliquiloculata</i>		1614	0	161	0.28	0.26	0.27	0.29			5.0	62%	0.20	0.17	1.68	0.011
O3711	OJP3711	<i>P. obliquiloculata</i>		3711	0	161	0.21	0.37	0.17	0.44			3.2	75%	0.09	0.11	0.84	0.004
	MW0691 4.5BC53																	
O4341	OJP4341	<i>P. obliquiloculata</i>		4341	0	162.2	0.72	0.13	0.75	0.29			4.8	81%	0.15	0.14	1.51	0.004
	MW0691 5.5BC58																	
O3420	OJP3420	<i>P. obliquiloculata</i>		3420	0	161	1.20	0.15	1.30	0.29			3.8	79%	0.06	0.05	0.65	0.004
	MW91-9 BC51																	
O4015	OJP4015	<i>P. obliquiloculata</i>		4015	0	161	1.85	0.19	2.09	0.34	-0.16	0.04	3.3	64%	0.09	0.06	0.84	0.006
	MW0691 5BC54																	
G4	G4	<i>P. obliquiloculata</i>	307727-307728	831	-28.4167	167.25	1.44	0.09	1.50	0.26	-0.04	0.04	7.8	59%	0.25	0.29	0.50	0.003
	G4	<i>T. crassaformis</i>	307720-307726	831	-28.4167	167.25	1.93	0.07	1.98	0.26	-0.08	0.05	16.5	68%	0.22	0.26	0.50	0.003
	G4	<i>T. truncatulinoides</i>	307733-307735	831	-28.4167	167.25	1.48	0.08	1.55	0.26	-0.15	0.05	8.3	64%	0.26	0.30	0.90	0.003
G4	G4	<i>O. universa</i>	307868	831	-28.4167	167.25	1.01	0.08	1.03	0.26			16.8	62%	0.22	0.23	0.03	0.002
T327	T327	<i>T. sacculifer</i> (mixed)	307870	1658	-11.505	174.5133	2.01	0.07	2.09	0.26	0.02	0.06	9.9	74%	0.20	0.20	0.74	0.009
T327#	T327#	<i>T. sacculifer</i> (mixed)	307870	1658	-11.505	174.5133	2.37	0.06	2.46	0.26			10.6	70%				

(Continues)

Table 2 (Continued)

Abbreviated Label	Original sample label	Species	Yale Peabody Museum #	Core-top Water depth (m)	Latitude	Longitude	$\delta^{53}\text{Cr}$ (%)	2 sigma internal <sup>a</sup>	853Cr blank corr. (%)	2 sigma external <sup>a</sup>	853Cr clay (%)	2 sigma internal used	Total Cr (ng)	Cr Yield <sup>b</sup>	Cr (ID) <sup>c</sup> ( $\mu\text{g g}^{-1}$ )	Cr (ICP-MS) ( $\mu\text{g g}^{-1}$ )	Ti (ICP-MS) ( $\mu\text{g g}^{-1}$ )	Cr/Mn
	T327	<i>G. siphonifera</i>	307863–307864	1658	–11.505	174.5133	2.02	0.07	2.09	0.26	–0.13	0.06	11.9	68%	0.24	0.28	1.12	0.005
C18P	CIRC02AR-018P	<i>N. ditertrei</i>	307876	2000	7.917	119.05	0.78	0.07	0.80	0.26		0.06	9.7	58%	0.16	0.17	0.91	0.002
	CIRC02AR-018P	<i>O. universa</i>	307875	2000	7.917	119.05	0.13	0.12	0.11	0.26		0.06	7.8	51%	0.27	0.28	0.08	0.003
	CIRC02AR-018P	<i>T. sacculifer</i> (mixed)	307877	2000	7.917	119.05	0.15	0.06	0.14	0.26		0.06	16.2	60%	0.60	0.57	0.15	0.003
	CIRC02AR-018P	<i>M. menardii</i>	307878	2000	7.917	119.05	0.47	0.04	0.47	0.26		0.04	27.5	77%	0.21	0.22	0.70	0.002
North Arabian Sea CD145	CD145 AI50	<i>O. universa</i>		151	23.27	66.7	0.60	0.06	0.60	0.26	–0.06	0.08	19.6	50%	0.83	0.85	0.21	0.009
	CD145 AI50#	<i>O. universa</i>		151	23.27	66.7	0.62	0.06	0.63	0.26		0.06	16.8	57%	0.85			

<sup>a</sup>External uncertainty is based on replicated USGS standard or internal uncertainty, whichever is greater.

<sup>b</sup>Cr yield through two column procedures. The matrix cut of the first column step was passed through the same column again; the Cr cuts from the two column procedures are combined.

<sup>c</sup>Cr concentration based on isotope dilution method.

purification method (modified from Bonnard, Parkinson, James, Karjalainen, & Fehr, 2011) to purify Cr from the matrix. Columns with an internal diameter (ID) of 8 mm (Diposaflex Polypropylene, Kimble Chase) filled with 4.3 ml AG50W-X8 resin were prepared and cleaned according to procedures outlined in Table 4. About 30 min prior to loading onto columns, the samples (dissolved in 0.5 ml 6N HCl) were taken off the hotplate and diluted with 5.5 ml 18.2 MΩ water to reach 0.5 N HCl, before being passed through the preconditioned columns. Chromium is eluted from the resin using 0.5 N HCl. Columns were then cleaned with 6 N HCl and 18.2 MΩ water and stored for reuse. The Cr recovery through one such AG50W-X8 resin step was only ~40%–60%. To enhance the recovery, the matrix cuts containing the residual Cr were passed through the same columns again. The Cr cuts from two column passes were combined.

Small quantities of Ti, V, and Fe will cause isobaric interferences on Cr isotope measurement by ICP-MS (Table 5). Because foraminiferal calcite contains very low levels of Cr and thus has very low tolerance to interference, even tiny amounts of these interference elements need to be removed. To remove the trace amount of Ti and V, samples were passed through a microcolumn (ID = 3 mm) filled with 0.3 ml AG50W-X8 resin (200–400 mesh size, Bio-Rad) according to procedures in Table 4 (modified from Trinquier, Birck, & Allègre, 2008). Finally, any remaining Fe was removed by passing the sample through a microcolumn (ID = 3 mm) filled with 0.3 ml AG1-X8 resin (100–200 mesh size, Bio-Rad) according to procedures outlined in Table 4. Purified Cr samples were finally dissolved in 0.5–1 ml 0.75 M HNO<sub>3</sub> for isotope measurement.

### 2.3. | MC-ICP-MS analysis

We used a Thermo Neptune Plus MC-ICP-MS housed at the Yale Metal Geochemistry Center equipped with a Pfeiffer OnToolBooster 150 Jet Pump that enables the usage of a Jet sampler cone and an X skimmer cone to maximize ion transmission efficiency. An Apex IR introduction system (Elemental Scientific) was used to further boost the signal intensity. With this setup, a sensitivity of  $8 \times 10^{-12}$  ampere was routinely achieved from a 10 ng g<sup>-1</sup> Cr solution at 50 μl min<sup>-1</sup> flow rate at high resolution ( $R \approx 10,000$ , see Weyer & Schwieters, 2003 for definition of mass resolution), which translates to ~0.05% ion transmission efficiency. The high mass resolution resolves polyatomic interferences <sup>40</sup>Ar<sup>12</sup>C, <sup>40</sup>Ar<sup>14</sup>N, and <sup>40</sup>Ar<sup>16</sup>O from <sup>52</sup>Cr, <sup>54</sup>Cr, and <sup>56</sup>Fe, respectively, but cannot resolve <sup>50</sup>Ti and <sup>50</sup>V from <sup>50</sup>Cr and <sup>54</sup>Fe from <sup>54</sup>Cr. Therefore, isotopes <sup>49</sup>Ti, <sup>51</sup>V, and <sup>56</sup>Fe are measured and used to correct <sup>50</sup>Ti, <sup>50</sup>V, and <sup>54</sup>Cr using <sup>50</sup>Ti/<sup>49</sup>Ti, <sup>50</sup>V/<sup>51</sup>V, and <sup>56</sup>Fe/<sup>54</sup>Fe ratios of 0.9586, 0.0024, and 15.6979, respectively, based on their natural abundances. Titanium and iron corrections were less than 0.05‰ and 0.5‰, respectively, which translate to negligible errors on final  $\delta^{53}\text{Cr}$  values.

Masses of 49, 50, 51, 52, 53, 54, and 56 are simultaneously measured on faraday cups connected to 10<sup>11</sup> Ω amplifiers (Table 5). Measurements consisted 5 block of 50 cycles, with each cycle lasting 4.19 s. Samples were bracketed with spiked standards (NIST SRM 979) of similar Cr concentrations, and on-peak blank was measured and subtracted from each sample and standard

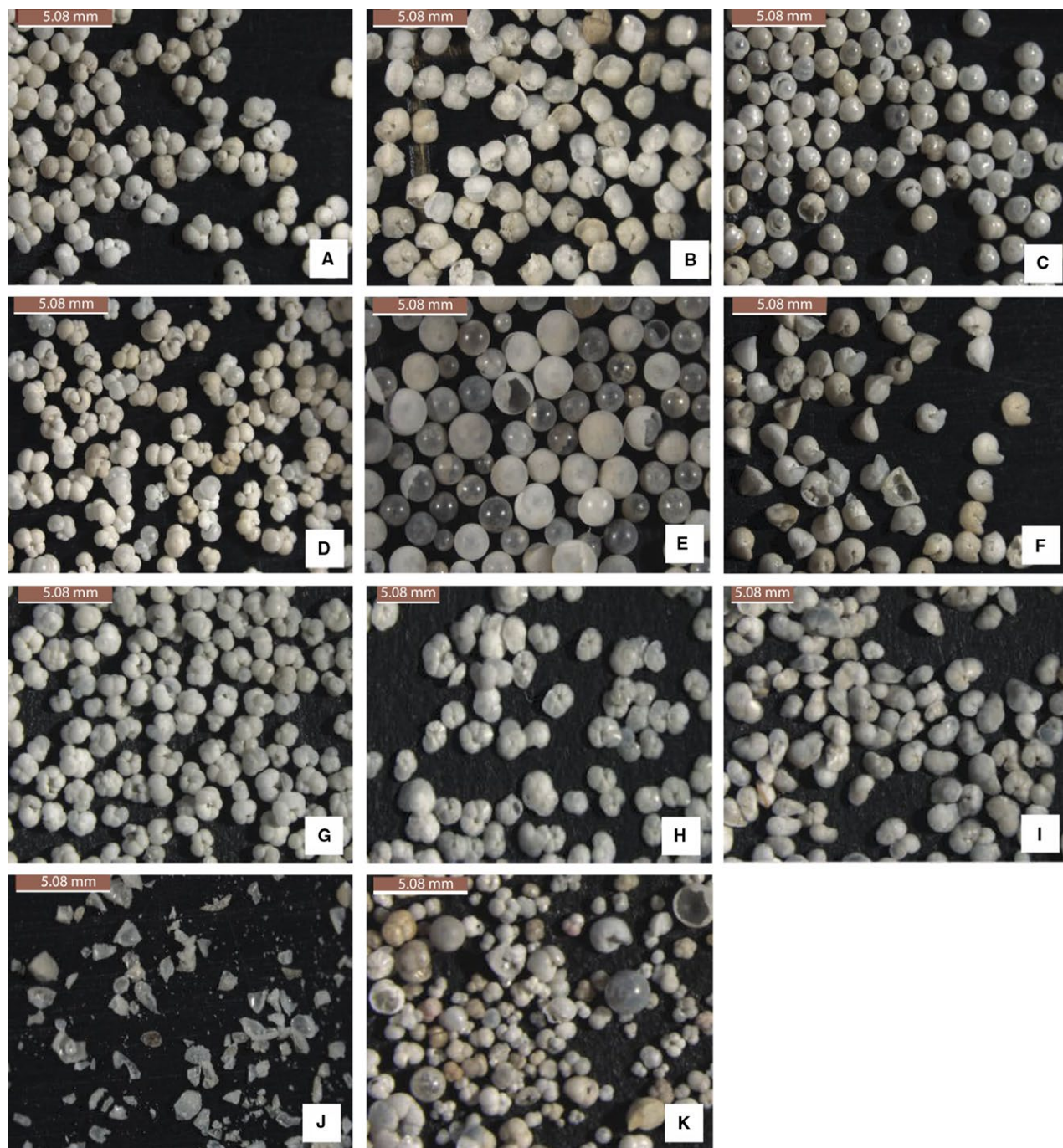


**FIGURE 2** Images of investigated species. (A) Yale Peabody Museum (YPM) 307871 *Trilobatus sacculifer* from KC26; (B) YPM 307720 *Truncorotalia crassaformis* from G4; (C) YPM 307727 *Pulleniatina obliquiloculata* from G4; (D) YPM 307863 *Globigerinella siphonifera* from T327; (E) YPM 307869 *Orbulina universa* from KC78; (F) YPM 307733 *Truncorotalia truncatulinoides* from G4; (G) YPM 307876 *Neogloboquadrina dutertrei* from CIRCO02AR-18P; (H) YPM 307878 *Menardella menardii* from CIRCO2AR-18P; (I) YPM 307872 *Globorotalia tumida* from KC26; (J) an example of shattered but not pulverized foraminifera chambers; (K) bulk foraminifera from VM-20-248. Foraminiferal species concepts after Kennett and Srinivasan (1983), with names updated to Aze et al. (2011) and Spezzaferri et al. (2015)

(blank–standard–blank–smp–blank–standard–blank) before double spike calculation. The blank-subtracted data are reduced using an iterative method to extract true sample  $^{53}\text{Cr}/^{52}\text{Cr}$  ratios, following methods described in Johnson, Herbel, Bullen, and Zawislanski (1999). Extracted  $^{53}\text{Cr}/^{52}\text{Cr}$  ratios are converted to  $\delta^{53}\text{Cr}$  by normalizing to standard SRM 979.

## 2.4 | Data quality

Data quality was verified by repeat measurements of procedural blanks, unprocessed SRM 979 and processed USGS geostandards (Tables 6 and 7). Unprocessed SRM 979 standards (Fig. 3A) that were used to bracket the samples yielded  $\delta^{53}\text{Cr}$  of  $-0.06 \pm 0.26\%$ ,

**TABLE 3** Results for testing the amount of Cr adsorbed to clay particles. Foraminifera chambers were crushed—without pulverizing—between two glass slides and then washed twice with 18.2 MΩ water. The two washes were combined, and the total desorbed Cr was measured

Sample label	Species	Cr mass (ng) in foram	Cr mass (ng) in rinse water	Percentage of foram Cr out of total Cr (%)
KC26	<i>M. menardii</i>	5.9	<DL	>98
CIRCO2AR-018P	<i>M. menardii</i>	27.5	<DL	>99
G4	<i>O. universa</i>	16.8	<DL	>99
KC26	<i>G. tumida</i>	25.9	0.5	96
KC26	<i>O. universa</i>	11.3	1.2	91
CIRCO2AR-018P	<i>N. dutertrei</i>	9.7	1.6	86
CIRCO2AR-018P	<i>T. sacculifer (mixed)</i>	16.2	0.4	97
CIRCO2AR-018P	<i>O. universa</i>	7.8	<DL	>98
KC26	<i>T. sacculifer (mixed)</i>	11.0	0.4	97
VM20-248	Bulk foram	19.7	2.2	90

**TABLE 4** Column procedures used to separate Cr from calcite matrix

Step	Reagent	Volume
Column 1: Extract Cr, 4.3 ml AG50W-X8 (200–400 mesh), column inner diameter 8 mm		
Clean resin	6 N HCl	4 × 10 ml
Clean resin	18.2 MΩ water	2 × 10 ml
Condition resin	0.5 N HCl	2 × 10 ml
Load samples and collect Cr	Dissolved in 0.5 N HCl	6 ml
Collect Cr	0.5 N HCl	4 ml
Clean resin	6 N HCl	2 × 10 ml
Clean resin	18.2 MΩ water	Full reservoir
Store resin in 0.1 N HCl		
Column 2: Remove V and Ti, 0.3 ml AG50W-X8 (200–400 mesh), column inner diameter ~3 mm		
Clean resin	0.5 N HF	2 × 2 ml
Clean resin	6 N HCl	2 × 2 ml
Clean resin	18.2 MΩ water	2 × 2 ml
Condition resin	0.5 N HNO <sub>3</sub>	2 ml
Load samples and collect Cr	Dissolved in 0.5 N HNO <sub>3</sub>	1 ml
Collect Cr	0.5 N HNO <sub>3</sub>	1 ml
Rinse Ti and V, discard eluent	0.5 N HF	2 ml
Rinse Ti and V, discard eluent	1 N HCl	2 × 3 ml
Collect Cr again and combine	2 N HCl	2 × 3 ml
Clean resin	18.2 MΩ water	Full reservoir
Store resin in 0.1 N HCl		
Column 3: Remove Fe, 0.3 ml AG1-X8 (100–200 mesh), column inner diameter ~3 mm		
Clean resin	3 N HNO <sub>3</sub>	4 ml
Clean resin	18.2 MΩ water	2 ml
Condition resin	6 N HCl	1 ml
Load samples and collect Cr	Dissolved in 6 N HCl	0.2 ml
Collect Cr	6 N HCl	0.4 ml
Clean resin	0.2 N HCl	2 × 2 ml
Clean resin	18.2 MΩ water	Full reservoir
Store resin in 0.1 N HCl		

measured at the concentrations (5–10 ppb) similar to or lower than samples. A secondary standard solution, NIST SRM 3112a (Table 7, Fig. 3B), with similar amount of Cr (5–20 ng) as in samples was processed through the same procedures as samples and yielded values ( $0.01 \pm 0.22\%$ ,  $n = 9$ ) consistent with previous measurements (Schoenberg et al., 2008). Completely dissolved USGS geostandards

BHVO-2 and BCR-2 (containing ~10–20 ng Cr) were also passed through the same column procedures as samples and also yielded values ( $-0.03 \pm 0.15\%$ ,  $n = 5$ , and  $-0.11 \pm 0.21\%$ ,  $n = 2$ , respectively) consistent within error with published values (Farkaš et al., 2013; Schoenberg et al., 2008). The 2 standard deviation of  $\delta^{53}\text{Cr}$  for the unprocessed SRM 979, processed SRM 3112a, processed

**TABLE 5** Faraday configuration for Cr isotope measurement on Neptune Plus MC-ICP-MS

Cup	L3	L2	L1	C	H1	H2	H4
Isotope	$^{49}\text{Ti}$	$^{50}\text{Ti}+^{50}\text{Cr}+^{50}\text{V}$	$^{51}\text{V}$	$^{52}\text{Cr}$	$^{53}\text{Cr}$	$^{54}\text{Cr}+^{54}\text{Fe}$	$^{56}\text{Fe}$

**TABLE 6** Measurements of Cr blanks. These blanks were contributed by three column procedures: two AG50W-X8 procedures to remove the majority of matrix, one AG50W-X8 procedure to remove trace Ti and V, and one AG1-X8 procedure to remove trace Fe

Sample	Cr mass (ng)	Yield (%)
Blank 1	0.7	82
Blank 2	0.5	81
Blank 3	0.4	78
Blank 4	0.4	51
Blank 5	0.3	72
Blank 6	0.3	84
Blank 7	0.6	68
Blank 8	0.5	91
Blank 9	0.6	83
Blank 10	0.7	54
Blank 11	0.2	127
Blank 12	0.1	66
Blank 13	0.6	73
Blank 14	0.6	69
Blank 15	0.7	85
Average	0.47	
2 SD	0.37	

BHVO-2, and processed BCR-2 were 0.26‰, 0.22‰, 0.15‰, and 0.21‰. Therefore, 0.26‰ is conservatively assigned as the external analytical uncertainty for samples. However, some samples with very low Cr (<5 ng) had >0.3‰ internal 2 standard error. We use whichever value is larger as an estimate of uncertainty. Although our full protocol errors are large relative to standard Cr isotope work (e.g., Bonnand et al., 2013; Ellis et al., 2002; Farkaš et al., 2013; Pereira et al., 2015; Scheiderich, Amini, Holmden, & Francois, 2015; Schoenberg et al., 2008; Wang, Reinhard et al., 2016) as a result of low [Cr] in foraminiferal carbonate, the error is small compared to the observed range in foraminiferal  $\delta^{53}\text{Cr}$  values.

Procedural blank contribution was assessed by repeatedly processing reagents through the same procedures as samples, with an average value of  $0.47 \pm 0.37$  ng ( $n = 15$ , Table 6). This blank level is higher than the 0.1–0.2 ng obtained by Bonnand et al. (2011), because we did the AG50W-X8 procedure twice (see ‘Sample preparation and chemical separation’ section) to enhance the yield, and because we added the necessary Ti-V-Fe removal procedures to remove these interferences. Even though the Cr blanks were very low, they were non-negligible, because sample Cr was also very low. Therefore, all samples were subject to blank correction using an empirically derived blank  $\delta^{53}\text{Cr}$  value of 0.41‰ (Table 7), although both uncorrected and corrected  $\delta^{53}\text{Cr}$

values are provided in Table 2. All foraminiferal  $\delta^{53}\text{Cr}$  values discussed in following sections are all blank-corrected.

### 3 | RESULTS

The Cr concentrations (Table 2) of investigated foraminiferal species range from 0.06 to 0.83  $\mu\text{g g}^{-1}$  (based on isotope dilution, which agrees well with ICP-MS measurements), with an average of 0.24  $\mu\text{g g}^{-1}$  ( $\pm 0.34$ , 2 SD). Chromium isotope results for all samples are presented in Table 2 and Fig. 5. The overall variation in  $\delta^{53}\text{Cr}$  of planktonic foraminifera is large with values ranging from  $\sim 0.1\%$  to  $\sim 2.5\%$ . In comparison, published seawater values range from  $\sim 0.4\%$  to 1.5‰ (Fig. 1). Detailed comparison between foraminifera and seawater is provided in the discussion section.

We find no correlation between  $\delta^{53}\text{Cr}$  and Cr/Ti (Fig. 4A) or between Cr and Ti concentrations in our samples (Fig. 4B). In addition, Cr-Ti data all plot above the upper continental crust line based on Rudnick & Gao, 2003 (Fig. 4B). All three lines of evidence suggest that the acetic acid leaching procedure predominantly released Cr from foraminiferal calcite, and not detrital clays. Furthermore, there are no systematic differences in either  $\delta^{53}\text{Cr}$  or Cr concentrations between samples cleaned for clays before leaching and those not cleaned. This suggests negligible Cr adsorbed to clay particles (Table 3). The residual clays surviving acetic acid leaching all returned  $\delta^{53}\text{Cr}$  values (Table 2) similar to the bulk silicate Earth (Farkaš et al., 2013; Schoenberg et al., 2008; Wang et al., 2016b). In addition, no correlation is observed between  $\delta^{53}\text{Cr}$  and Cr/Mn (Fig. 4C), suggesting a lack of significant oxide contamination.

### 4 | DISCUSSION

#### 4.1 | Cr uptake during calcification

Trace elements are incorporated into foraminiferal calcite from a reservoir of vacuolized, modified seawater (Elderfield, Bertram, & Erez, 1996; Erez, 2003). Foraminifera can raise the pH of this internal biomineralization reservoir to facilitate calcification (Bentov, Brownlee, & Erez, 2009), thereby modifying the concentration or isotopic composition of some geochemical proxies. It is possible that such biomineralization processes could have played important roles in modulating Cr uptake.

The total Cr concentrations in foraminiferal calcite from Atlantic and Pacific Oceans are 0.10–0.39  $\mu\text{g g}^{-1}$  and 0.06–0.60  $\mu\text{g g}^{-1}$ , respectively. Previously published average total Cr concentrations of seawater in Atlantic and Pacific seawater are 0.33 ng  $\text{g}^{-1}$  and

**TABLE 7** Measurements of secondary standards that were processed through the same procedures as samples. After brief measurement of each blank sample for isotope dilution calculation for blank Cr, the remaining of twelve individual blank solutions were combined to generate high enough Cr so that the isotopic composition of blank Cr could be estimated

Sample	$\delta^{53}\text{Cr}$	$2\sigma^a$	Yield	Cr mass used (ng)
Blank (combined)	0.41	0.26		~5
SRM 3112a (1)	-0.06	0.26	82%	10.4
SRM 3112a (2)	-0.10	0.26	84%	10.7
SRM 3112a (3)	-0.09	0.26	83%	10.9
SRM 3112a (4)	0.00	0.26	76%	10.5
SRM 3112a (5)	0.17	0.26	75%	5.7
SRM 3112a (6)	0.00	0.26	76%	5.7
SRM 3112a (7)	-0.08	0.26	66%	19.7
SRM 3112a (8)	0.05	0.26	63%	10.6
SRM 3112a (9)	0.19	0.26	46%	5.6
SRM 3112a mean	0.01			
SRM 3112a 2 SD	0.22			
BHVO-2 (1)	-0.14	0.26	76%	20.0
BHVO-2 (2)	-0.08	0.26	67%	20.9
BHVO-2 (3)	-0.02	0.26	53%	13.4
BHVO-2 (4)	0.04	0.26	53%	10.6
BHVO-2 (5)	0.03	0.26	46%	9.6
BHVO-22 mean	-0.03			
BHVO-22 2 SD	0.15			
BCR2 (1)	-0.03	0.26	62%	26.9
BCR2 (2)	-0.18	0.26	65%	9.3
BCR2 mean	-0.11			
BCR2 2 SD	0.21			

<sup>a</sup>Either internal 2 standard error or external 2 standard deviation of standards, whichever is greater.

0.15 ng g<sup>-1</sup>, respectively (Bonnand et al., 2013; Jeandel & Minster, 1984, 1987; Scheiderich et al., 2015). Therefore, the conservative estimate of the distribution coefficient ( $D_{\text{Cr}} = [\text{Cr}]_{\text{foram}}/[\text{Cr}]_{\text{seawater}}$ ) describing uptake of Cr in foraminifera from seawater ranges from ~300 to 4000. This distribution coefficient stands in sharp contrast, to previous experimentally determined  $D_{\text{Cr(VI)}}$  values for inorganic precipitation of calcite range from ~0.1 to ~3.4, depending on the Cr concentration in the solution phase (Rodler et al., 2015; Tang, Elzinga, Lee, & Reeder, 2007). The apparent much larger  $D_{\text{Cr}}$  values during foraminiferal calcification as compared to inorganic calcite precipitation points to important biological control on Cr uptake in planktonic foraminifera.

However, it is also unclear whether Cr is incorporated in to foraminiferal calcite as Cr(III) or as Cr(VI). During precipitation of inorganic calcite in previous experiments, Cr(VI) was incorporated into the calcite lattice without changing its valence state and this caused significant distortions to the calcite lattice structure (Tang et al., 2007). Given complex biomineralization pathways, it is possible that these inorganic uptake mechanisms may not be analogous in biogenic carbonates. At equilibrium, thermodynamics predict that Cr(VI) is the predominant oxidation state in the ocean (Elderfield, 1970; Pettine & Millero, 1990).

However, in waters with high dissolved organic content, up to ~50% of total Cr can be Cr(III), likely complexed with organic ligands [denoted as OM-Cr(III)] (e.g., Kaczynski & Kieber, 1994). The discrepancy between thermodynamic prediction and empirical observations can be explained by the slow kinetics of oxidation of Cr(III) to Cr(VI) without catalysis by manganese oxides (Van Der Weijden & Reith, 1982).

Because of the toxic nature of Cr(VI) and the particle-reactive nature of Cr(III) (Rai, Sass, & Moore, 1987), it is possible that Cr(III) is the phase incorporated into foraminiferal calcite. Indeed, a recent culture experiment found that Cr(III) uptake is significantly favored over Cr(VI) uptake by phytoplankton (Semeniuk, Maldonado, & Jaccard, 2016). However, Pereira et al. (2015) proposed that Cr(VI) may enter coral skeletons through a reductive and subsequent oxidative pathway that induces Cr isotope fractionation. The seawater and coral aragonite Cr concentrations measured by these authors at the Rocas Atoll (Tropical South Atlantic) yielded  $D_{\text{Cr}}$  values ranging from 127 to 289, which lie between those for foraminiferal calcite uptake and inorganic calcite precipitation. Both foraminifera (Erez, 2003) and corals (McCulloch, Falter, Trotter, & Montagna, 2012) precipitate calcium carbonate from an alkaline microenvironment, but the speed and specific mechanism of precipitation, and carbonate crystal structures (calcite in

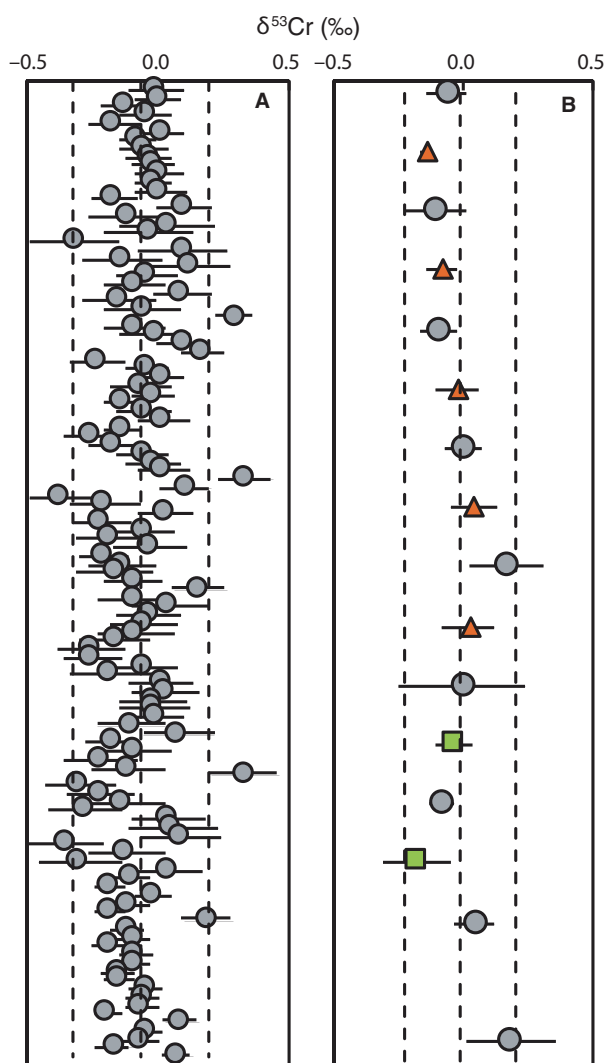


**FIGURE 3** Results for the unprocessed standard SRM 979 (A) that was used to bracket each sample at similar concentrations ( $5\text{--}10\text{ ng g}^{-1}$ ) and processed standard SRM 3112a (gray circles in B) and USGS basalt standards BHVO-2 (red triangles in B) and BCR-2 (green squares in B). Sample  $\delta^{53}\text{Cr}$  values were normalized to the average  $\delta^{53}\text{Cr}$  value of SRM 979 analyzed before and after each sample. The dashed lines in the figure delineate the 95% confidence interval around the mean ( $-0.06\text{‰} \pm 0.26\text{‰}$ ) for SRM 979, and ( $-0.02 \pm 0.19\text{‰}$ ) for the processed standards. For interpretation of the colors in this figure, the readers are referred to the web version of this article

foraminifera vs. aragonite in corals), may have lead to different distribution coefficients like those observed

## 4.2 | Heterogeneous seawater $\delta^{53}\text{Cr}$

Heterogeneous seawater  $\delta^{53}\text{Cr}$  provides a possible explanation for the large variability in foraminiferal  $\delta^{53}\text{Cr}$  among core-top species and samples. Published seawater  $\delta^{53}\text{Cr}$  values (Bonnand et al., 2013; Pereira et al., 2015; Scheiderich et al., 2015) suggest that  $\delta^{53}\text{Cr}$  values vary regionally, even over relatively short distances, and with depth by up to  $\sim 1\text{‰}$  and  $\sim 0.5\text{‰}$ , respectively (Fig. 1).

However, there is little consistency in existing seawater  $\delta^{53}\text{Cr}$  observations. For instance, variations in  $\delta^{53}\text{Cr}$  with water depth (0–2000 m) are evident in the Arctic but not in the South Atlantic Ocean (Bonnand et al., 2013; Scheiderich et al., 2015).

Given that the Cr residence time in the modern ocean ( $\sim 9000$  years, see Reinhard et al., 2014) is about ten times longer than the seawater mixing time ( $\sim 1000$  years, Broecker & Peng, 1982), one would expect that seawater Cr is reasonably mixed. Highly variable seawater  $\delta^{53}\text{Cr}$ , therefore, suggests there is active Cr cycling within the ocean with large associated Cr isotope fractionation. This is consistent with the previous observation of large variation in Cr concentration and speciation in the surface ocean (Jeandel & Minster, 1987 references compiled in Bonnand et al., 2013).

On the one hand, Cr(III) adsorbs readily to particles, and so can be efficiently scavenged in high productivity areas. Although negligible fractionation was observed during adsorption of Cr(VI) to iron and aluminum oxides under equilibrium conditions (Ellis et al., 2004), isotope effects during adsorption of Cr(III) have not been explored and could be important.

Reduction of Cr(VI) to Cr(III), on the other hand, could induce large and variable isotope fractionation, depending on the types of reductants and reduction kinetics (Basu & Johnson, 2012; Basu, Johnson, & Sanford, 2014; Døssing et al., 2011; Ellis et al., 2002; Kitchen et al., 2012; Pereira et al., 2015; Scheiderich et al., 2015). Because of this, Scheiderich et al. (2015) proposed that Cr(VI) to Cr(III) reduction is the primary factor leading to heterogeneous seawater  $\delta^{53}\text{Cr}$  values. Future studies of global seawater and river water systems including suspended particles are needed to fully understand the global distribution of seawater  $\delta^{53}\text{Cr}$  heterogeneity.

In summary, both foraminiferal calcite and seawater have highly heterogeneous  $\delta^{53}\text{Cr}$ , with differing patterns of variability in both systems. Globally heterogeneous seawater  $\delta^{53}\text{Cr}$  may be attributed to variable Cr redox cycling in the mixed layer. In addition, both Cr(III) and Cr(VI) occur in seawater, and each may have their own  $\delta^{53}\text{Cr}$  signatures and be incorporated into foraminifera calcite at different proportions. These factors make it difficult, at this point, to compare foraminiferal  $\delta^{53}\text{Cr}$  data to limited published seawater data measured for total Cr. Even so, a few general patterns can still be recognized from our foraminifera data (below).

## 4.3 | Comparison between foraminiferal and seawater $\delta^{53}\text{Cr}$

In the North Atlantic (Fig. 1), *O. universa* (mixed layer to thermocline habitat) (Fig. 5) from four core tops gave  $\delta^{53}\text{Cr}$  values ranging from  $0.4\text{‰}$  to  $0.9\text{‰}$ . The observed  $0.4\text{--}0.9\text{‰}$   $\delta^{53}\text{Cr}$  in the same foraminiferal species suggests  $\sim 0.5\text{‰}$  variability in seawater  $\delta^{53}\text{Cr}$  in this region, or an environmental effect size of  $\sim 0.5\text{‰}$  variation on chromium isotope incorporation into foraminiferal calcite. This variability is within the range of surface waters analyzed in the North Pacific, Arctic, and Argentine Basin (Scheiderich et al., 2015), although lower than the single North Atlantic seawater measurement of  $1.5\text{‰}$  at Southampton (Bonnand et al., 2013). However,

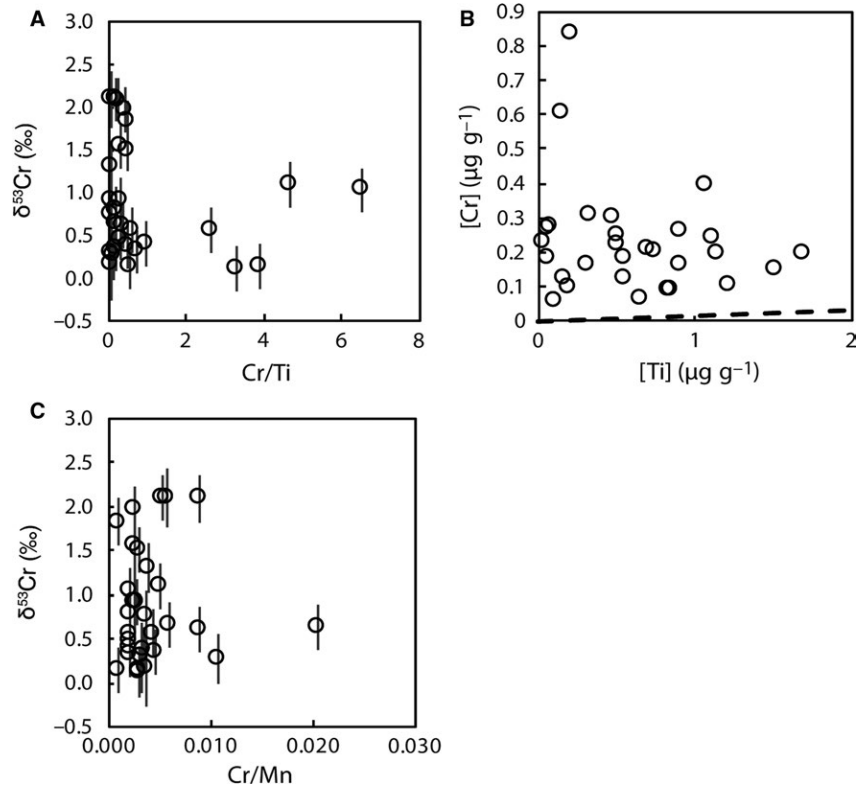


**FIGURE 4** Results for  $\delta^{53}\text{Cr}$  and Cr-Ti-Mn concentrations for the investigated foraminifera species. The dashed line in B represents the Cr-Ti relationship for the upper continental crust (Rudnick & Gao, 2003). All Cr-Ti data points plot well above the upper continental trend, suggesting that the weak acetic acid leaching did not introduce contamination from detrital sources. Lack of correlation in C suggests insignificant contamination from oxides

the Southampton sample is unlikely to be representative of North Atlantic seawater as it was sampled at 12 m depth in the coastal sea that discharges into the English Channel.

In the Central Atlantic, four species and one bulk foraminiferal sample yielded  $\delta^{53}\text{Cr}$  values ranging from 0.1‰ to 1.1‰ (Fig. 5). This range is lower than, or similar to the Central Atlantic surface seawater range of  $\sim 0.9\text{‰}$ – $1.0\text{‰}$  (Pereira et al., 2015; Scheiderich et al., 2015). There is no systematic difference in chromium isotopes between mixed layer (*T. sacculifer*) and mixed layer to thermocline species (*O. universa*, *G. tumida*, *M. menardii*). However, in core-top KC26 (dated to be Holocene, Crotese et al., in prep) *O. universa* is isotopically heavier than the shallower species *T. sacculifer*, which is inconsistent with either the Arctic (decrease with depth, Scheiderich et al., 2015) or Argentine Basin (no change, Bonnard et al., 2013) seawater depth profile.

In the West Pacific and North Arabian Sea, eight species yielded  $\delta^{53}\text{Cr}$  values from 0.1‰ to 2.5‰. Unfortunately, there are no seawater  $\delta^{53}\text{Cr}$  data published so far in these regions to compare with our foraminifera values. However, several patterns could still be recognized. First, significant  $\delta^{53}\text{Cr}$  variability ( $\sim 0.2\text{‰}$ – $2.1\text{‰}$ ) is observed in the same species, *P. obliquiloculata*, from adjacent core tops. Second, in core-top G4 sample (dated to be 945 year BP by  $^{14}\text{C}$ , Sun et al., 2006), species with shallower habitat depths (*O. universa* and *P. obliquiloculata*) yielded  $\delta^{53}\text{Cr}$  values lower than species with deeper habitat depths (*T. truncatulinooides* and *T. crassaformis*). Similar patterns with depth are also observed in core-top CIRCO2AR-018P. Although seawater depth profile in the West Pacific Ocean is still lacking, there is no obvious reason to have increasing  $\delta^{53}\text{Cr}$  with water depth, as

current observation is that either seawater  $\delta^{53}\text{Cr}$  decreases with water depth (Arctic seawater depth profile, Scheiderich et al., 2015) or there is no significant variation (Argentine Basin, Bonnard et al., 2013).

In summary, the lack of *in situ* seawater  $\delta^{53}\text{Cr}$  data precludes confident comparisons between foraminiferal calcite and seawater  $\delta^{53}\text{Cr}$  values. However, the large interspecies variation in  $\delta^{53}\text{Cr}$  within the same core-top sample, together with opposing depth trends to expected seawater values, points to biological controls on Cr isotope fractionation during foraminiferal calcification.

#### 4.4 | Biological control on foraminiferal $\delta^{53}\text{Cr}$

When considering the possibility of Cr isotope fractionation during foraminiferal calcification, it is tempting to compare to previous inorganic calcite precipitation experiments and coral aragonite measurements. Previous experimental precipitation of inorganic calcite found  $\sim 0.3\text{‰}$  fractionation at high [Cr], but negligible isotope fractionation at low [Cr] similar to those in seawater (Rodler et al., 2015). However, as in other isotope systems (e.g., Noireaux et al., 2015), observed fractionations in inorganic precipitates may not necessarily be directly applicable to biological systems. As mentioned before, biologically mediated Cr isotope fractionations of  $\sim -0.6$  to  $-1.4\text{‰}$  are evident during coral aragonite precipitation (Pereira et al., 2015). The direction of Cr isotope fractionation in corals is broadly consistent with that in foraminifera. That is, their  $\delta^{53}\text{Cr}$  values are generally lower than those in the ambient seawater. However, the variations in corals measured so far appear to be narrower than foraminifera.

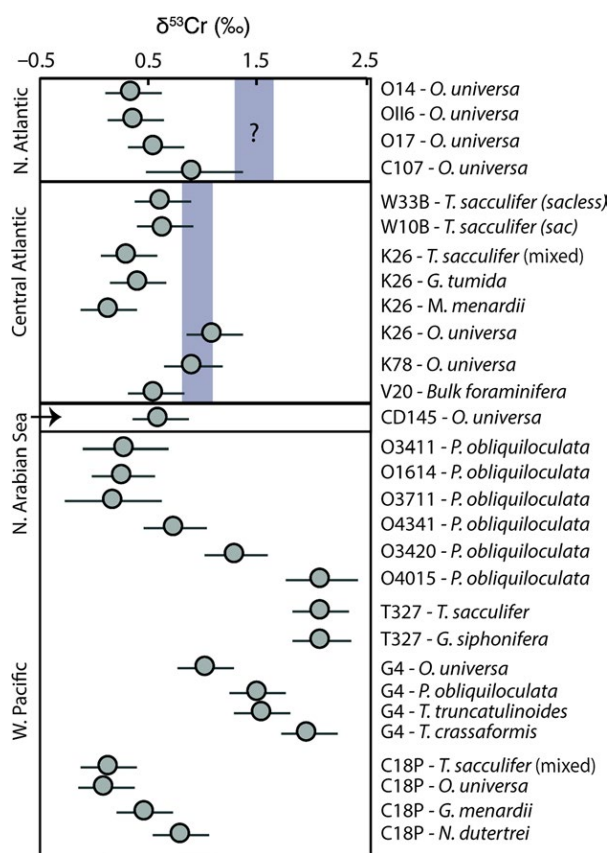


**FIGURE 5** The  $\delta^{53}\text{Cr}$  results for all samples examined in this study. Each bin represents a region as noted on the left side of the frame (circles in Fig. 1). The species from each region is plotted from top to bottom according to their habitat depth (e.g., *T. sacculifer* is a shallow species and thus is plotted on top of the bins). Sample names are given on the right side of the frame (see Table 2 for full station names). The gray bars represent available seawater data in the region (seawater data sources: Bonnand et al., 2013; Frei et al., 2014; Pereira et al., 2015; Scheiderich et al., 2015). Note that the gray bars represent only limited seawater data and thus may not represent the true range in the region; especially, the N Atlantic seawater is based on only one data from Southampton shallow coastal water. None of the investigated species seem to consistently match with limited seawater values in each region. This likely indicates significant Cr isotope fractionation during foraminiferal calcite precipitation and/or much more heterogeneous seawater  $\delta^{53}\text{Cr}$  values than previously thought

The apparent variability of foraminiferal  $\delta^{53}\text{Cr}$  values could also be due to variable Cr uptake mechanisms. In regions with high dissolved organic matter, foraminifera could preferentially uptake OM-Cr(III), as observed for some phytoplankton (Semeniuk et al., 2016). In regions where dissolved organic concentration is low, foraminifera may switch to the reductive Cr(VI) uptake mechanism, as proposed for coral growth (Pereira et al., 2015). As Cr(III) is typically isotopically lighter than Cr(VI) in both equilibrium and kinetic fractionations (e.g., Ellis et al., 2002; Schauble et al., 2004; Wang, Johnson, & Ellis, 2015), the OM-Cr(III) uptake mechanism would lead to relatively low  $\delta^{53}\text{Cr}$  values. A reductive Cr(VI) uptake mechanism is also expected to lead to lower-than-seawater  $\delta^{53}\text{Cr}$  values in foraminiferal calcite, but the exact  $\delta^{53}\text{Cr}$  value depends on the extent of reduction and specific

metabolism. A small extent of reduction would lead to low  $\delta^{53}\text{Cr}$  values while quantitative reduction would lead to similar to seawater values.

## 5 | CONCLUDING REMARKS

Due to lack of *in situ* seawater  $\delta^{53}\text{Cr}$  data to compare with our foraminifera data, we could not conclude which foraminiferal species, if any, could be used as a reliable proxy of seawater  $\delta^{53}\text{Cr}$ . However, we observed large  $\delta^{53}\text{Cr}$  variations between species within and among samples. The variation in  $\delta^{53}\text{Cr}$  among different samples could be explained by heterogeneous seawater  $\delta^{53}\text{Cr}$ . However, we also find that species with similar depth habitats from the same core-top sample also yielded different  $\delta^{53}\text{Cr}$  values. In addition, within samples, shallower species yielded consistently lower  $\delta^{53}\text{Cr}$  than deeper species, which is opposite to the general patterns expected in seawater  $\delta^{53}\text{Cr}$  (Bonnand et al., 2013; Scheiderich et al., 2015). These observations indicate that biology could play a major role in controlling Cr isotope fractionation during foraminiferal calcification. However, more surface seawater and depth profile data, ideally from sites where foraminiferal  $\delta^{53}\text{Cr}$  data are available, are needed to better understand these biological effects.

It is notable that the  $\sim 2.5\%$   $\delta^{53}\text{Cr}$  variation observed across all samples presented here is comparable to that observed in deep time shale and iron formation samples measured so far (Cole et al., 2016; Gueguen et al., 2016; Planavsky, Reinhard et al., 2014; Reinhard et al., 2014; Schoenberg et al., 2008; Wang et al., 2016a; Wang, Reinhard et al., 2016; Wille et al., 2013). In Precambrian rocks, reported  $\delta^{53}\text{Cr}$  values range from  $\sim -1\%$  to  $\sim +2\%$  (Crowe et al., 2013; Frei & Polat, 2012; Frei et al., 2009; Planavsky, Asael et al., 2014; Planavsky, Reinhard et al., 2014). In Phanerozoic samples, reported  $\delta^{53}\text{Cr}$  values range from  $\sim -0.6\%$  to  $\sim +5\%$  (Berger & Frei, 2014; Frei et al., 2009, 2014; Pereira et al., 2015; Planavsky, Asael et al., 2014; Reinhard et al., 2014; Wang et al., 2016a). Therefore, when using planktonic foraminiferal  $\delta^{53}\text{Cr}$  to reconstruct seawater redox, interspecific biological fractionation and the possibility of highly heterogeneous surface seawater  $\delta^{53}\text{Cr}$  must be considered. Future field work, including plankton tows coupled with *in situ* seawater measurement, or laboratory culturing experiments, may shed more light on this issue.

A final note is that if variability in planktonic foraminifera stems from highly heterogeneous surface seawater  $\delta^{53}\text{Cr}$ , it suggests active and fast Cr cycling within the surface ocean. As a result, even if certain foraminifera species could record seawater  $\delta^{53}\text{Cr}$  without fractionation (as may be the case with *Orbulina universa* in North Atlantic), given shallow seawater  $\delta^{53}\text{Cr}$  heterogeneity, Cr isotope data from one site would only inform local seawater redox conditions. If the deep ocean is less heterogeneous than surface seawater, as suggested by published Atlantic and Pacific data (Bonnand et al., 2013; Scheiderich et al., 2015), epifaunal benthic foraminifera might still potentially serve as robust benthic redox proxies, provided sample size requirements could be sufficiently reduced to make such measurements feasible.

## ACKNOWLEDGMENT

This work is funded by Agouron Institute to X.W. A.T received funding (BES grant DE-FG02-13ER16402 and a LabEx International Research Chair) from the 'Laboratoire d'Excellence' LabexMER (ANR-10-LABX-19), co-funded by a grant from the French government under the program 'Investissements d'Avenir'. The authors wish to thank the Ocean Drilling Program, Helen Bostock (NIWA, NZ), Bruce Corliss (Graduate School of Oceanography, University of Rhode Island), and Richard Norris (Scripps Institution of Oceanography, University of California San Diego) for providing core-top sediments.

## REFERENCES

- Aze, T., Ezard, T. H., Purvis, A., Coxall, H. K., Stewart, D. R., Wade, B. S., & Pearson, P. N. (2011). A phylogeny of Cenozoic macroperforate planktonic foraminifera from fossil data. *Biological Reviews*, *86*, 900–927.
- Barling, J., & Anbar, A. (2004). Molybdenum isotope fractionation during adsorption by manganese oxides. *Earth and Planetary Science Letters*, *217*, 315–329.
- Basu, A., & Johnson, T. M. (2012). Determination of hexavalent chromium reduction using Cr stable isotopes: Isotopic fractionation factors for permeable reactive barrier materials. *Environmental Science & Technology*, *46*, 5353–5360.
- Basu, A., Johnson, T. M., & Sanford, R. A. (2014). Cr isotope fractionation factors for Cr (VI) reduction by a metabolically diverse group of bacteria. *Geochimica et Cosmochimica Acta*, *142*, 349–361.
- Bé, A., & Tolderlund, D. (1971). Distribution and ecology of living planktonic foraminifera in surface waters of the Atlantic and Indian Oceans. In B.M. Funnell, W.R. Riedel (Eds.), *The Micropaleontology of Oceans*, (pp.105–149). Cambridge: Cambridge University Press.
- Bentov, S., Brownlee, C., & Erez, J. (2009). The role of seawater endocytosis in the biomineralization process in calcareous foraminifera. *Proceedings of the National Academy of Sciences*, *106*, 21500–21504.
- Berger, A., & Frei, R. (2014). The fate of chromium during tropical weathering: A laterite profile from Central Madagascar. *Geoderma*, *213*, 521–532.
- Bonnand, P., James, R., Parkinson, I., Connelly, D., & Fairchild, I. (2013). The chromium isotopic composition of seawater and marine carbonates. *Earth and Planetary Science Letters*, *382*, 10–20.
- Bonnand, P., Parkinson, I. J., James, R. H., Karjalainen, A.-M., & Fehr, M. A. (2011). Accurate and precise determination of stable Cr isotope compositions in carbonates by double spike MC-ICP-MS. *Journal of Analytical Atomic Spectrometry*, *26*, 528–535.
- Broecker, W., & Peng, T. (1982). *Tracers in the Sea*. Palisades, NY, USA: Lamont-Doherty Geol. Obs.
- Cole, B. C., Gueguen, B., Wang, X., Reinhard, C., Halverson, G. P., Lyons, T., & Planavsky, N. (2016). A shale-hosted Cr isotope record of low atmospheric oxygen during the Proterozoic. *Geology*, doi: 10.1130/G37787.1 [Epub ahead of print].
- Cortese, G., & Prebble, J. (2015). A radiolarian-based modern analogue dataset for palaeoenvironmental reconstructions in the Southwest Pacific. *Marine Micropaleontology*, *118*, 34–49.
- Crowe, S. A., Døssing, L. N., Beukes, N. J., Bau, M., Kruger, S. J., Frei, R., & Canfield, D. E. (2013). Atmospheric oxygenation three billion years ago. *Nature*, *501*, 535–538.
- Døssing, L., Dideriksen, K., Stipp, S., & Frei, R. (2011). Reduction of hexavalent chromium by ferrous iron: A process of chromium isotope fractionation and its relevance to natural environments. *Chemical Geology*, *285*, 157–166.
- Eary, L. E., & Rai, D. (1987). Kinetics of chromium (III) oxidation to chromium (VI) by reaction with manganese dioxide. *Environmental Science & Technology*, *21*, 1187–1193.
- Elderfield, H. (1970). Chromium speciation in sea water. *Earth and Planetary Science Letters*, *9*, 10–16.
- Elderfield, H., Bertram, C., & Erez, J. (1996). A biomineralization model for the incorporation of trace elements into foraminiferal calcium carbonate. *Earth and Planetary Science Letters*, *142*, 409–423.
- Ellis, A. S., Johnson, T. M., & Bullen, T. D. (2002). Chromium isotopes and the fate of hexavalent chromium in the environment. *Science*, *295*, 2060.
- Ellis, A. S., Johnson, T. M., & Bullen, T. D. (2004). Using chromium stable isotope ratios to quantify Cr (VI) reduction: Lack of sorption effects. *Environmental Science & Technology*, *38*, 3604–3607.
- Erez, J. (2003). The source of ions for biomineralization in foraminifera and their implications for paleoceanographic proxies. *Reviews in Mineralogy and Geochemistry*, *54*, 115–149.
- Farkaš, J., Chrastny, V., Novak, M., Cadkova, E., Pasava, J., Chakrabarti, R., ... Bullen, T. D. (2013). Chromium isotope variations ( $\delta^{53/52}\text{Cr}$ ) in mantle-derived sources and their weathering products: Implications for environmental studies and the evolution of  $\delta^{53/52}\text{Cr}$  in the Earth's mantle over geologic time. *Geochimica et Cosmochimica Acta*, *123*, 74–92.
- Fendorf, S. E., & Zasoski, R. J. (1992). Chromium (III) oxidation by  $\delta\text{-MnO}_2$ . *Environmental Science & Technology*, *26*, 79–85.
- Frei, R., Gaucher, C., Poulton, S. W., & Canfield, D. E. (2009). Fluctuations in Precambrian atmospheric oxygenation recorded by chromium isotopes. *Nature*, *461*, 250–253.
- Frei, R., Poiré, D., & Frei, K. M. (2014). Weathering on land and transport of chromium to the ocean in a subtropical region (Misiones, NW Argentina): A chromium stable isotope perspective. *Chemical Geology*, *381*, 110–124.
- Frei, R., & Polat, A. (2012). Chromium isotope fractionation during oxidative weathering-implications from the study of a Paleoproterozoic (ca. 1.9 Ga) paleosol, Schreiber Beach, Ontario, Canada. *Precambrian Research*, *224*, 434–453.
- Gueguen, B., Reinhard, C. T., Algeo, T. J., Peterson, L., Nielsen, S., Wang, X. L., & Planavsky, N. J. (2016). The chromium isotope composition of reducing and oxic marine sediments. *Geochimica et Cosmochimica Acta*, *184*, 1–19.
- Hemleben, C., Spindler, M., & Anderson, O. R. (2012) *Modern planktonic foraminifera*. New York: Springer Science & Business Media.
- Henehan, M. J., Rae, J. W., Foster, G. L., Erez, J., Prentice, K. C., Kucera, M., ... Wilson, P. A. (2013). Calibration of the boron isotope proxy in the planktonic foraminifera *Globigerinoides ruber* for use in palaeo-CO<sub>2</sub> reconstruction. *Earth and Planetary Science Letters*, *364*, 111–122.
- Hirst, D., & Nicholls, G. (1958). Techniques in sedimentary geochemistry: (1) Separation of the detrital and non-detrital fractions of limestones. *Journal of Sedimentary Research*, *28*, 468–481.
- Hutchins, D. A., & Bruland, K. W. (1998). Iron-limited diatom growth and Si:N uptake ratios in a coastal upwelling regime. *Nature*, *393*, 561–564.
- Jeandel, C., & Minster, J.-F. (1984). Isotope dilution measurement of inorganic chromium (III) and total chromium in seawater. *Marine Chemistry*, *14*, 347–364.
- Jeandel, C., & Minster, J. (1987). Chromium behavior in the ocean: Global versus regional processes. *Global Biogeochemical Cycles*, *1*, 131–154.
- Johnson, T. M., Herbel, M. J., Bullen, T. D., & Zawislanski, P. T. (1999). Selenium isotope ratios as indicators of selenium sources and oxyanion reduction. *Geochimica et Cosmochimica Acta*, *63*, 2775–2783.
- Kaczynski, S. E., & Kieber, R. J. (1994). Hydrophobic C18 bound organic complexes of chromium and their potential impact on the geochemistry of Cr in natural waters. *Environmental Science & Technology*, *28*, 799–804.
- Keeling, R. F., Körtzinger, A., & Gruber, N. (2010). Ocean deoxygenation in a warming world. *Annual Reviews of Marine Science*, *2*, 199–229.
- Kennett, J. P., & Srinivasan, M. (1983) *Neogene planktonic foraminifera: A phylogenetic atlas*. Stroudsburg: Hutchinson Ross.
- Kitchen, J. W., Johnson, T. M., Bullen, T. D., Zhu, J., & Raddatz, A. (2012). Chromium isotope fractionation factors for reduction of Cr(VI) by aqueous Fe(II) and organic molecules. *Geochimica et Cosmochimica Acta*, *89*, 190–201.

- Konhauser, K. O., Lalonde, S. V., Planavsky, N. J., Pecoits, E., Lyons, T. W., Mojzsis, S. J., ... Fralick, P. W. (2011). Aerobic bacterial pyrite oxidation and acid rock drainage during the Great Oxidation Event. *Nature*, *478*, 369–373.
- Lenton, T. M., & Watson, A. J. (2000). Redfield revisited: 1. Regulation of nitrate, phosphate, and oxygen in the ocean. *Global Biogeochemical Cycles*, *14*, 225–248.
- Martin, J.-M., & Meybeck, M. (1979). Elemental mass-balance of material carried by major world rivers. *Marine Chemistry*, *7*, 173–206.
- Mcculloch, M., Falter, J., Trotter, J., & Montagna, P. (2012). Coral resilience to ocean acidification and global warming through pH up-regulation. *Nature Climate Change*, *2*, 623–627.
- Müller, P. J., & Suess, E. (1979). Productivity, sedimentation rate, and sedimentary organic matter in the oceans—I. Organic carbon preservation. *Deep Sea Research Part A. Oceanographic Research Papers*, *26*, 1347–1362.
- Noireaux, J., Mavromatis, V., Gaillardet, J., Schott, J., Montouillout, V., Louvat, P., ... Neuville, D. (2015). Crystallographic control on the boron isotope paleo-pH proxy. *Earth and Planetary Science Letters*, *430*, 398–407.
- Pereira, N. S., Vögelin, A. R., Paulukat, C., Sial, A. N., Ferreira, V. P., & Frei, R. (2015). Chromium-isotope signatures in scleractinian corals from the Rocas Atoll, Tropical South Atlantic. *Geobiology*, *4*, 1–13.
- Pettine, M., & Millero, F. J. (1990). Chromium speciation in seawater: The probable role of hydrogen peroxide. *Limnology and Oceanography*, *35*, 730–736.
- Planavsky, N. J., Asael, D., Hofmann, A., Reinhard, C. T., Lalonde, S. V., Knudsen, A., ... Rouxel, O. J. (2014). Evidence for oxygenic photosynthesis half a billion years before the Great Oxidation Event. *Nature Geoscience*, *7*, 283–286.
- Planavsky, N. J., Reinhard, C. T., Wang, X., Thomson, D., MCGoldrick, P., Rainbird, R. H., ... Lyons, T. W. (2014). Low Mid-Proterozoic atmospheric oxygen levels and the delayed rise of animals. *Science*, *346*, 635–638.
- Rai, D., Sass, B. M., & Moore, D. A. (1987). Chromium(III) hydrolysis constants and solubility of chromium(III) hydroxide. *Inorganic Chemistry*, *26*, 345–349.
- Reinhard, C. T., Planavsky, N. J., Robbins, L. J., Partin, C. A., Gill, B. C., Lalonde, S. V., Bekker, A., Konhauser, K. O., & Lyons, T. W. (2013). Proterozoic ocean redox and biogeochemical stasis. *Proceedings of the National Academy of Sciences of the United States of America*, *110*, 5357–5362.
- Reinhard, C. T., Planavsky, N. J., Wang, X., Fischer, W. W., Johnson, T. M., & Lyons, T. W. (2014). The isotopic composition of authigenic chromium in anoxic marine sediments: A case study from the Cariaco Basin. *Earth and Planetary Science Letters*, *407*, 9–18.
- Rodler, A., Sánchez-Pastor, N., Fernández-Díaz, L., & Frei, R. (2015). Fractionation behavior of chromium isotopes during coprecipitation with calcium carbonate: Implications for their use as paleoclimatic proxy. *Geochimica et Cosmochimica Acta*, *164*, 221–235.
- Rudnick, R. L., & Gao, S. (2003). Composition of the continental crust. In K. Turekian, & H. D. Holland (Eds.), *Treatise on geochemistry* (pp. 1–64). Oxford: Pergamon.
- Salomons, W., & Förstner, U. (1980). Trace metal analysis on polluted sediments: Part II: Evaluation of environmental impact. *Environmental Technology*, *1*, 506–517.
- Schauble, E., Rossman, G. R., & Taylor, H. P. Jr (2004). Theoretical estimates of equilibrium chromium-isotope fractionations. *Chemical Geology*, *205*, 99–114.
- Scheiderich, K., Amini, M., Holmden, C., & Francois, R. (2015). Global variability of chromium isotopes in seawater demonstrated by Pacific, Atlantic, and Arctic Ocean samples. *Earth and Planetary Science Letters*, *423*, 87–97.
- Schoenberg, R., Zink, S., Staubwasser, M., & Von Blanckenburg, F. (2008). The stable Cr isotope inventory of solid Earth reservoirs determined by double spike MC-ICP-MS. *Chemical Geology*, *249*, 294–306.
- Semeniuk, D., Maldonado, M. T., & Jaccard, S. L. (2016). Chromium uptake and adsorption in cultured marine phytoplankton-implications for the marine Cr cycle. *Geochimica et Cosmochimica Acta*, *184*, 41–54.
- Silvester, W. (1989). Molybdenum limitation of symbiotic nitrogen fixation in forests of Pacific Northwest America. *Soil Biology and Biochemistry*, *21*, 283–289.
- Spero, H. J., Lerche, I., & Williams, D. F. (1991). Opening the carbon isotope "vital effect" black box, 2. Quantitative model for interpreting foraminiferal carbon isotope data. *Paleoceanography*, *6*, 639–655.
- Spezzaferri, S., Kucera, M., Pearson, P., Wade, B., Rappo, S., Poole, C., ... Stalder, C. (2015). Fossil and genetic evidence for the polyphyletic nature of the planktonic foraminifera "globigerinoides", and description of the new genus *trilobatus*. *PLoS ONE*, *10*, e0128108.
- Sun, X., Corliss, B. H., Brown, C. W., & Showers, W. J. (2006). The effect of primary productivity and seasonality on the distribution of deep-sea benthic foraminifera in the North Atlantic. *Deep Sea Research Part I: Oceanographic Research Papers*, *53*, 28–47.
- Tang, Y., Elzinga, E. J., Lee, Y. J., & Reeder, R. J. (2007). Coprecipitation of chromate with calcite: Batch experiments and X-ray absorption spectroscopy. *Geochimica et Cosmochimica Acta*, *71*, 1480–1493.
- Trinquier, A., Birck, J.-L., & Allègre, C. J. (2008). High-precision analysis of chromium isotopes in terrestrial and meteorite samples by thermal ionization mass spectrometry. *Journal of Analytical Atomic Spectrometry*, *23*, 1565–1574.
- Tripati, A. K., Eagle, R. A., Thiagarajan, N., Gagnon, A. C., Bauch, H., Halloran, P. R., & Eiler, J. M. (2010). 13C-18O isotope signatures and 'clumped isotope' thermometry in foraminifera and coccoliths. *Geochimica et Cosmochimica Acta*, *74*, 5697–5717.
- Van Cappellen, P., & Ingall, E. D. (1996). Redox stabilization of the atmosphere and oceans by phosphorus-limited marine productivity. *Science*, *271*, 493–496.
- Van Der Weijden, C., & Reith, M. (1982). Chromium (III)—chromium (VI) interconversions in seawater. *Marine Chemistry*, *11*, 565–572.
- Wang, X. L., Johnson, T. M., & Ellis, A. S. (2015). Equilibrium isotopic fractionation and isotopic exchange kinetics between Cr (III) and Cr (VI). *Geochimica et Cosmochimica Acta*, *153*, 72–90.
- Wang, X. L., Planavsky, N. J., Reinhard, C. T., Zou, H., Ague, J. J., Wu, Y., ... Peucker-Ehrenbrink, B. (2016a). Chromium isotope fractionation during subduction-related metamorphism, black shale weathering, and hydrothermal alteration. *Chemical Geology*, *429*, 19–33.
- Wang, X. L., Planavsky, N. J., Reinhard, C. T., Zou, H. J., Ague, J. J., Wu, Y. B., ... Peucker-Ehrenbrink, B. (2016b). Chromium isotope fractionation during subduction-related metamorphism, black shale weathering, and hydrothermal alteration. *Chemical Geology*, *423*, 19–33.
- Wang, X. L., Reinhard, C., Planavsky, N., Owens, J. D., Lyons, T., & Johnson, C. M. (2016). Sedimentary chromium isotopic compositions across the Cretaceous OAE2 at Demerara Rise Site 1258. *Chemical Geology*, *429*, 85–92.
- Weyer, S., & Schwieters, J. (2003). High precision Fe isotope measurements with high mass resolution MC-ICP-MS. *International Journal of Mass Spectrometry*, *226*, 355–368.
- Wille, M., Nebel, O., Van Kranendonk, M. J., Schoenberg, R., Kleinhanns, I. C., & Ellwood, M. J. (2013). Mo-Cr isotope evidence for a reducing Archean atmosphere in 3.46–2.76 Ga black shales from the Pilbara, Western Australia. *Chemical Geology*, *340*, 68–76.